Korean J. of Chem. Eng., **14**(2), 117-124 (1997)

EFFECT OF DIFFUSION AND CONVECTION ON THE FLUX OF DEPOSITING PARTICLES NEAR A PREADSORBED PARTICLE

Ho Suk Choi† **and Julian Talbot***

School of Chemical Engineering, Chungnam National University, Taejon 305-764, Korea
*Department of Chemistry and Biochemistry, Duquesne University, Pittsburgh, PA 15282-1503, USA
(Received 11 October 1996 • accepted 11 February 1997)

Abstract – A steady state convective-diffusion equation is solved using a collocation method to find the concentration profile and flux of adsorbing particles near a particle adsorbed on a line. At small values of the gravity number, $N_G=\pi d^4 \Delta\rho g/6kT$, the concentration profile and flux vary slowly near the preadsorbed particle, while they are highly non-uniform at large values of N_G. The numerical results are compared with Brownian dynamics simulation for a range of N_G values. The effect of the position of the system boundary on the collocation calculation is discussed and it is shown how the concept of flux balance may be used to improve the accuracy of the results. Finally, we develop a truncated power series that accurately fits the numerical data.

Key words: *Particle Deposition, Sedimentation, Diffusion, RSA, Brownian Dynamics*

INTRODUCTION

The adsorption of macromolecules such as latexes, proteins, bacteria and enzymes plays an important role in many different industrial fields, including chromatographic separation, filtration, water cleansing and biofouling [Andrade, 1985, 1987; Andrade and Hlady, 1987]. Despite their importance, the theoretical analysis of these processes is still at the beginning stage. Although the Langmuir theory is widely used to describe adsorption processes, it assumes that the size of the solute particles is much smaller than the spacing of binding sites on the solid substrate. This is true in the cases referred to above since each solute particle randomly covers and bonds with many active sites on the substrate. Consequently, the surface blocking effect of preadsorbed particle is very important and has to be taken into account. The adsorption of biomacromolecules is usually regarded as a random and (partially) irreversible process. Due to these special features, classical equilibrium thermodynamic approaches can not be applied to this adsorption process.

In the random sequential adsorption (RSA) process particles are adsorbed randomly and sequentially on a plain substrate and fixed at the initially adsorbed place if they do not overlap with preadsorbed particles. The kinetics of the model [Schaaf and Talbot, 1989] and the structure of deposited particles have been studied. In particular, the saturation coverage [Feder, 1980; Hinrichsen et al., 1986], $\theta_\infty=0.547...$, is in good agreement with the experimental estimate (0.55 ± 0.01) of Onoda and Liniger [1986] for the deposition of latex spheres.

Although the RSA model successfully describes the random, irreversible and blocking nature of the adsorption process, it does not properly incorporate the transport mechanism of the particles from bulk to substrate. To incorporate this realistic situation in the case where the density difference between solute and solvent is not significant, the diffusion random sequential adsorption (DRSA) model [Senger et al., 1991, 1992, 1993], based upon sequential Brownian dynamics simulation, has been developed. Many adsorption configurations are built up by a number of independent random walks from the bulk phase to the surface. Remarkably, the structure, as characterized by the radial distribution function, and the coverage of jammed configuration generated by DRSA model were found to be indistinguishable from those of simple RSA [Senger et al., 1992, 1993; Bafaluy et al., 1995]. This reflects that, although it does not take into account the proper transport mechanisms, RSA can still be a valid model in situations where the particle dynamics is controlled by diffusion.

On the other hand, when the density between solute and solvent is large, the adsorbing particles follow straight line instead of Brownian trajectories. To describe this situation the ballistic deposition (BD) model [Talbot and Ricci, 1992] was developed in which particles are dropped to the surface, and are accepted if they are not blocked by preadsorbed particles or if there is room near the blocking particles. In the latter case, the particles roll down the surface of the preadsorbed particles [Talbot and Ricci, 1992; Thompson and Glandt, 1992; Choi et al., 1993]. In BD, since the effect of nonuniform adsorption is quite significant, the kinetics and the structure of particle deposits are significantly different from those of RSA and DRSA.

In a real system, the density difference between particles and solvent may be between the two extremes: a diffusion controlled process and a gravity controlled process. Besides, other factors, such as temperature and the particle size, will affect the transport mechanism of particle from bulk solution to surface. Senger et al. [1992, 1993] have studied the effect of both diffusion and gravity on the adsorption of hard spheres after fixing the temperature of system and the density difference between solvent and solute, and successfully obtained the jamming coverages for particle with different sizes. However, the sequential

†To whom correspondence should be addressed.

Brownian dynamic simulation which they used has several drawbacks including the expense and the uncertainty which results from the use of a finite mesh and the starting point of the diffusing particles. Thus, the primary objective of this study is to develop a more efficient simulation method which provides accurate flux distributions of adsorbing particles. The secondary objective is to develop an accurate fitting function for the numerical results. In this study, we do not take into account the effect of hydrodynamic interactions and colloidal forces.

FORMULATION OF THE TRANSPORT EQUATION

When the density of the adsorbing particle is larger than that of solvent, one should take into account the effect of convection due to gravity as well as that of diffusion. In this case, the governing steady state convective-diffusion equation [Elimelech, 1994a; 1994b] becomes, with the assumption of constant diffusivity and no inter-particle interactions,

$$\nabla^2 c - \nabla \cdot \left(\frac{\mathbf{F}}{kT} c\right) = 0, \tag{1}$$

where c is the concentration of the particles in the solution phase, **F** the force vector acting on a particle, k the Boltzmann constant, and T is the temperature of system. If we use the diameter of a particle, d, as a length scale and denote by c_0 the particle concentration in the bulk phase, the above equation can be non-dimensionalized:

$$\nabla^2 \Psi - \nabla \cdot \left(\frac{\mathbf{F}d}{kT} \Psi\right) = 0, \tag{2}$$

where Ψ is the normalized concentration distribution of particles in solution phase:

$$\Psi = \frac{c}{c_0}. \tag{3}$$

The flux at position **r** is

$$\mathbf{J}(\mathbf{r}) = -D \cdot \nabla \Psi + \frac{\mathbf{D} \cdot \mathbf{F}}{kT} d\Psi. \tag{4}$$

For deposition onto an empty surface, Eq. (2) becomes

$$\frac{d^2\Psi}{dy^2} + N_G \frac{d\Psi}{dy} = 0, \tag{5}$$

where

$$N_G = \frac{\pi d^4 \Delta\rho g}{6kT} \tag{6}$$

is the dimensionless *gravity number* which is the product of the Peclet number, $N_{Pe} \equiv \frac{3\pi\mu d^2 U}{2kT}$, and the sedimentation number, $N_S \equiv \frac{d^2 \Delta\rho g}{18\,\mu U}$, that is $N_G = 2N_{Pe}N_S$. With $\Psi(0)=0$ and $\Psi(\infty)=1$, the solution is

$$\Psi = 1 - e^{-N_G y} \tag{7}$$

and the flux at the surface is

$$J = -D\frac{\partial c}{\partial y}\Big|_{y=0} = -Dc_0\frac{\partial \Psi}{\partial y}\Big|_{y=0} = -Dc_0 N_G. \tag{8}$$

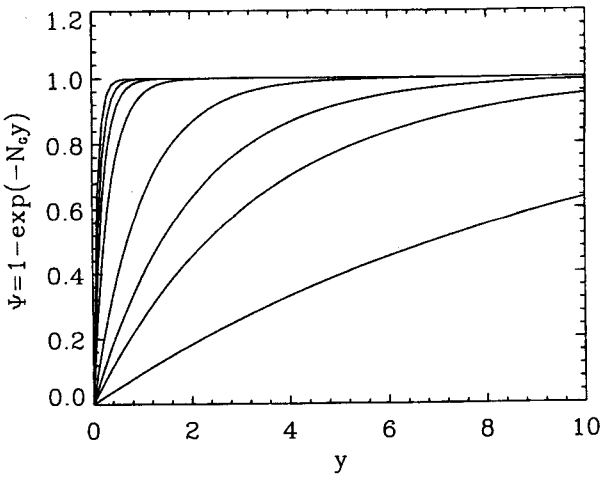

Fig. 1. Normalized concentration distribution of incoming particles near the surface at steady state without any interference of preadsorbed particles. The solid lines correspond to different gravity numbers: N_G=0.1, 0.3, 0.5, 1.0, 3.0, 5.0, 7.0, 10.0 from bottom to top.

As expected, the flux increases with increasing N_G. Fig. 1 shows the concentration profiles at different values of N_G and represents the probability distribution of incoming particles near the surface at steady state. As expected, the rate of adsorption increases with increasing gravity number. As the size or the density of particles increases, the adsorption rate increases. When N_G is close to zero, the concentration of particles increases slowly to the bulk concentration, but, as N_G increases, the concentration of particles rapidly approaches the bulk concentration just above the substrate surface. This means that the layer between surface and the bulk phase becomes smaller as $N_G \to \infty$ and, as $N_G \to 0$, the overall concentration profile theoretically becomes zero (Fig. 1). This means that the irreversible adsorption can take place even without any bulk concentration difference because the particle dynamics is controlled by local density difference, in other words, Brownian dynamics.

To obtain the rate of arrival of the adsorbing particles near a preadsorbed particle in a 1+1 D system, it is convenient to use the coordinate system shown in Fig. 2. The diffusion equation then becomes

$$\frac{\partial^2\Psi}{\partial r^2} + \left(\frac{1}{r} + N_G \sin\theta\right)\frac{\partial \Psi}{\partial r} + \frac{1}{r^2}\frac{\partial^2 \Psi}{\partial \theta^2} + N_G \frac{\cos\theta}{r}\frac{\partial \Psi}{\partial \theta} = 0, \tag{9}$$

with boundary conditions

$$\Psi = 0, \quad \text{at } y=0, \tag{10}$$

$$\frac{\partial \Psi}{\partial r} + N_G \sin\theta\, \Psi = 0, \quad \text{at } r=1, \tag{11}$$

$$\frac{\partial \Psi}{\partial \theta} = 0, \quad \text{at } \theta = 0, \tag{12}$$

$$\Psi = \Psi_0 = 1 - \exp(-N_G r_0 \sin\theta) \quad \text{at } r = r_0. \tag{13}$$

Eq. (11) represents a reflecting boundary at the surface of the preadsorbed sphere, Eq. (12) imposes the symmetry requirement and Eq. (13) reflects the fact that the concentration profile far

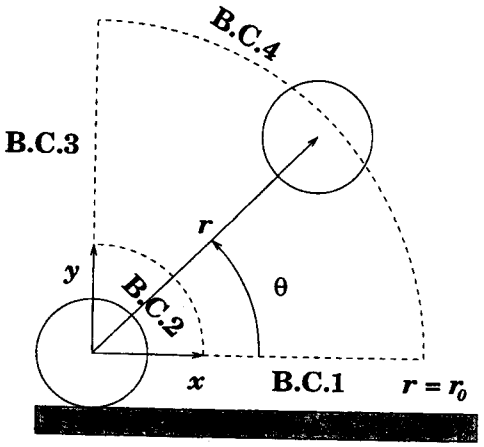

Fig. 2. System boundary represented in the cylindrical coordinate system.

from a preadsorbed particle is given by the undisturbed solution, Eq. (7).

For a sphere depositing on a plane in the presence of a preadsorbed particle we use a spherical coordinate system with azimuthal symmetry. The governing steady state diffusion equation Eq. (2) takes the form

$$\frac{\partial^2\Psi}{\partial r^2}+\left(\frac{2}{r}+N_G\sin\theta\right)\frac{\partial\Psi}{\partial r}+\frac{1}{r^2}\frac{\partial^2\Psi}{\partial\theta^2}-\left(\frac{\tan\theta}{r^2}-N_G\frac{\cos\theta}{r}\right)\frac{\partial\Psi}{\partial\theta}=0, \tag{14}$$

where we have again assumed constant diffusivity and no interparticle interactions. The boundary conditions are the same as in the 1+1 D system.

NUMERICAL ANALYSIS

Eq. (9) does not possess analytical solutions. Numerical solutions, however, may be conveniently and rapidly obtained with a collocation procedure. To apply the method, the region of interest is first mapped to a square region and we select $n_c \times n_c$ collocation points at the nodes of a square lattice (In *orthogonal* collocation, the collocation points are already determined from the roots of Jacobi-Polynomial. The method has the advantage of accuracy at the collocation points but also the disadvantage of inflexibility since we can not choose the collocation points as we want.).

The numerical solution is represented as a linear combination of Lagrange polynomials with unknown coefficients. Substitution of these functions in the differential equation yields a residual function and the unknown coefficients are determined by setting the residual functions equal to zero at the collocation points. The complete concentration profile may then be obtained by interpolating between the collocation points. Full details of the method are presented in the Appendix.

After obtaining a set of converged solutions, we can calculate the flux of particles at the interface by differentiating the probability function:

$$J(r)\Big|_{y=0}=-D\left(\frac{\partial c}{\partial y}\right)_{y=0}=-Dc_0\left(\frac{\partial\Psi}{\partial y}\right)_{y=0}, \tag{15}$$

where **r** is the position on the surface relative to the center of the preadsorbed particle.

In order to understand the influence of the preadsorbed sphere, it is convenient to divide the solution into two parts:

$$\Psi=\Psi_0+\Psi_1, \tag{16}$$

where Ψ_0 is the steady state distribution of particles when the surface is empty and Ψ_1 is the perturbation induced by a preadsorbed particle. From Eq. (8), Eq. (15) and Eq. (16), we have the following equation:

$$J(r)=J_0+J_1(r), \tag{17}$$

where

$$J_0=-Dc_0N_G \tag{18}$$

is the flux on an empty surface and J_1, therefore, shows the effects of lateral diffusion relative to convection due to gravity.

We have found that the flux J_1 should satisfy a normalization condition which we now derive. Since the total flux to the surface must be the same with and without a preadsorbed particle we have in the 1+1 D system that

$$\int_1^\infty J(x)\,dx=\int_0^\infty J_0\,dx, \tag{19}$$

where we take a lower limit of one on the left hand side corresponding to the particle diameter since there is no flux within the exclusion region of the adsorbed particle. Inserting Eq. (18) into Eq. (19) yields

$$\int_1^\infty \frac{J_1(x)}{J_0}dx=1. \tag{20}$$

In the 2+1 D system, the equivalent relationship is

$$2\int_1^\infty \frac{J_1(r)}{J_0}r\,dr=1. \tag{21}$$

In this paper, we assume the diffusion coefficient D is constant but it really depends on the viscosity of fluid and the distance between particles and the substrate [Pagonabaraga and Rubí, 1994]. And, also, we does not take into account the effect of van der Waals and double-layer forces between particles. The effect of hydrodynamic and colloidal interactions on the deposition process is investigated elsewhere [Pagonabaraga and Rubi, 1994].

BROWNIAN DYNAMICS SIMULATION

In order to confirm the effectiveness of collocation method, we have used the Brownian dynamic simulation. The general idea of the simulation has already been explained elsewhere [Senger et al., 1991, 1992]. In this section, we present the key details. In 1+1 D system under the influence of gravity, the jump probabilities of a particle from its position to one of four adjacent nodes are:

$$P(x^+)=P(x^-)=\frac{1}{2+\exp(\delta N_G/4R)+\exp(-\delta N_G/4R)} \tag{22}$$

$$P(y^+)=\frac{\exp(-\delta N_G/4R)}{2+\exp(\delta N_G/4R)+\exp(-\delta N_G/4R)} \quad (23)$$

$$P(y^-)=\frac{\exp(+\delta N_G/4R)}{2+\exp(\delta N_G/4R)+\exp(-\delta N_G/4R)} \quad (24)$$

where δ is the jump distance and x^+ denotes a jump of one step in the positive x direction, etc. Each particle starts at a randomly chosen point in a plane at a height equal to 3R. According to the probability of making a step, the trajectory of a particle is determined. Once it hits the surface, it is fixed but if it continuously diffuses away from the surface, it is rejected.

In 2+1 D system, particles can jump to one of six adjacent nodes. The corresponding probabilities are simply modified as follows:

$$P(x^+)=P(x^-)=P(z^+)=P(z^-)=\frac{1}{4+\exp(\delta N_G/4R)+\exp(-\delta N_G/4R)} \quad (25)$$

$$P(y^+)=\frac{\exp(-\delta N_G/4R)}{4+\exp(\delta N_G/4R)+\exp(-\delta N_G/4R)} \quad (26)$$

$$P(y^-)=\frac{\exp(+\delta N_G/4R)}{4+\exp(\delta N_G/4R)+\exp(-\delta N_G/4R)}. \quad (27)$$

RESULTS

1. Probability of Finding an Incoming Particle near a Preadsorbed Particle

The probability distribution, Ψ, of the position of the center of the diffusing particle at steady state is shown in Fig. 3. The black pie represents the preadsorbed particle and the gray quarter annulus represents area excluded to the center of an incoming sphere. The lines are contours of constant concentration normalized by the bulk value. The contour plot at low gravity number, Fig. 3(a), shows a slowly varying distribution of particles consistent with diffusion controlled dynamics. As the gravity number increases, the overall adsorption rate also increases and the adsorption rate of particles in the vicinity of a preadsorbed particle is larger than that far away from the preadsorbed particle (see Fig. 4). When N_G=1.0 [Fig. 3(b)], the concentration profile varies rapidly and one can observe the accumulation of particle density just above the preadsorbed particle. When N_G=2, 5 [Fig. 3(c) and (d)], the biased distribution becomes dominant and so intense that the denser concentration profile is observed in the vicinity of the preadsorbed particle. The four figures taken together show qualitatively the transition between a diffusion controlled process and a convection dominated process due to gravity. As the gravity number increases, the bulk phase moves closer to the surface. Thus, even in the absence of the preadsorbed particle, the probability distribution becomes very steep. When N_G=5, the bulk phase approaches around y=2 at x=4.

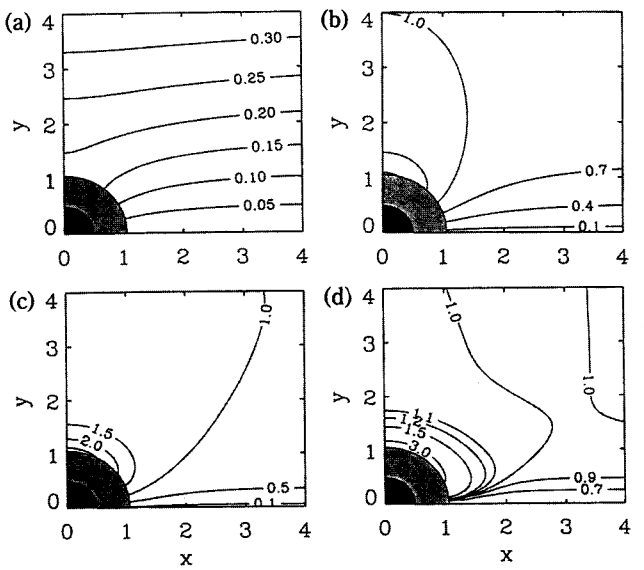

Fig. 3. Probability distribution of finding an incoming particle near a preadsorbed particle in 1+1 D system. Lines represent contour plots of probability distribution of particles. (a) N_G=0.1 , (b) N_G=1.0 , (c) N_G= 2.0, (d) N_G=5.0.

2. Correction of Numerical Results

The numerical solution is sensitive to both the number of collocation points (n_c) and the location of the system boundary (r_0).

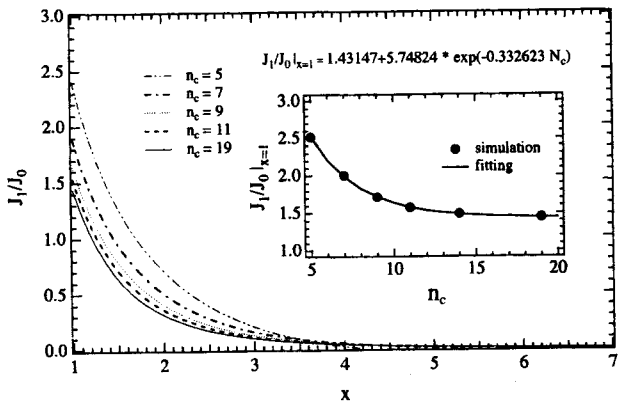

Fig. 4. Dependence of local flux distributions, J_1/J_0, on the number of collocation points. The insert shows the effect of varying the number of collocation points on the flux at x=1 .

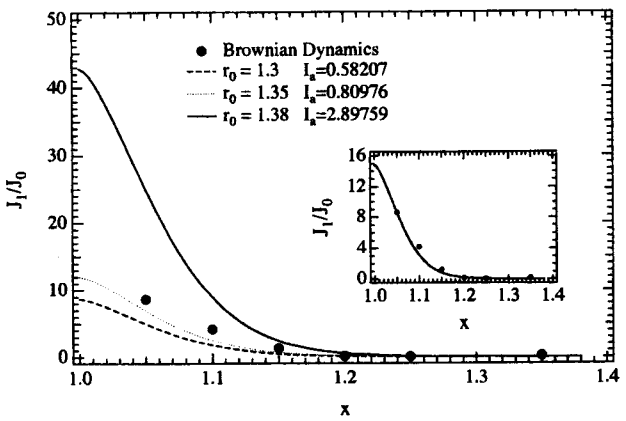

Fig. 5. Effect of the location of the system boundary on the local flux distribution. In the insert, solutions of Brownian dynamic simulation show good agreement with numerical solutions obtained after normalization of the fluxes calculated by the collocation method.

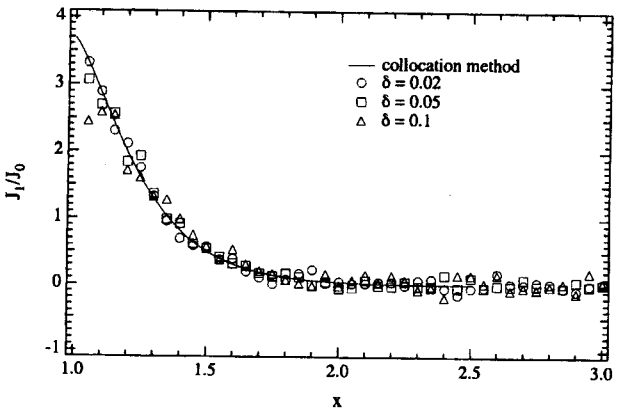

Fig. 6. Comparison of the normalized flux distribution with solutions of Brownian dynamic simulations using different values of mesh sizes.

Fig. 4 shows the effect of varying n_c. In this calculation, N_G=1 and r_0=10. The insert represents the change of flux just near preadsorbed particle with increasing n_c. When many collocation points are used, as the figure shows, numerical solutions asymptotically approach the true solution. When $n_c \geq 19$, reasonable numerical solutions can be obtained. The fitting function of the small figure shows that $J_1/J_0|_{x=1} \rightarrow 1.43147$ as $n_c \rightarrow \infty$.

Fig. 5 shows the change of flux distribution with different locations of the system boundary, r_0, when N_G=100 and n_c=19. When N_G is large, the numerical solutions sensitively depend on r_0. As shown in the figure, the flux distribution is overestimated for r_0=1.38 and it is underestimated when r_0 is 1, 3 or 1.35. This effect results from the fact that we assume the undisturbed boundary condition at an arbitrary position, r=r_0. But, we can correct these fluxes by applying the flux balance (19). As a result of normalization using Eq. (20), three fluxes are transformed into one flux distribution as shown in the insert of Fig. 5. Thus, this correction procedure using the concept of flux balance can remove possible errors which may result from the numerical analysis.

3. Effectiveness of Collocation Method

Fig. 6 compares the particle flux distributions obtained by collocation with those obtained by Brownian dynamics simulation. When δ=0.02 in the Brownian dynamics simulation, the two results show good agreement. In the cases of δ=0.05, 0.1, however, the Brownian dynamics results show large local fluctuations of fluxes. Large deviations between two results are observed near preadsorbed particle if insufficient lattice spacing is used. The accuracy of numerical solutions obtained from Brownian dynamic simulation sensitively depends on the number of independent simulations as well as on the size of lattice spacing. Table 1 compares the calculation conditions of two methods. For the comparison, a workstation (Sparc 20) was used. For example, the collocation method is 13 times faster than the Brownian dynamics simulation when δ=0.02.

4. Particle Flux Distributions Near a Preadsorbed Particle

Fig. 7 shows the effect of gravity number on the normalized flux, J_1/J_0. As N_G increases, the convection due to gravity controls the dynamics of adsorbing particles and the lateral diffusion becomes relatively weaker. Fig. 7 also supports the general argument that lateral diffusion favors a uniform distribution of particles on the surface, although even when N_G=0 the adsorption is non-uniform due to geometric blocking. Thus, at large values of N_G, the perturbation is restricted to the immediate vicinity of the adsorbed particle and the flux distribution function approaches a delta function at x=1. When an adsorbing particle follows a pure Brownian dynamics trajectory (N_G=0) from the bulk phase to the surface near a preadsorbed particle, it can move any direction with equal probability through the bulk phase and hit the surface of a preadsorbed particle. As a result of this reflection from the surface of the preadsorbed particle, diffusing particles accumulate near the preadsorbed particle. However, as N_G increases, the diffusing particles have a bias under the field. This difference of particle movements leads to varying rates of arriving particles onto the surface near a preadsorbed particle as displayed in Fig. 7. As expected, the adsorption rate is more intense near a preadsorbed particle as the gravity number increases.

Table 1. Comparison of computing times of collocation method and Brownian dynamic simulation

Simulation methods / Comparison	Collocation method	Brownian dynamic simulation (100 independent runs)		
	N_G=10 n_c=19	δ=0.02	δ=0.05	δ=0.1
Time (sec)	58	754	122	31

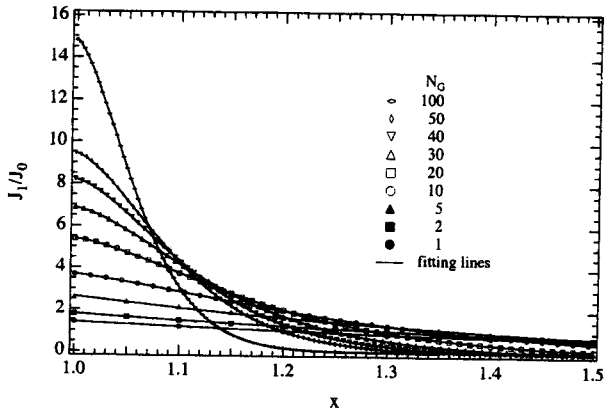

Fig. 7. Normalized flux distributions calculated at different values of N_G.

We have attempted to fit the numerically obtained flux distributions. We are guided in the choice of function by the analytic result for no diffusion [Slattery, 1981], N_G=0. In this case,

$$J = J_0\left(1+\frac{1}{x^2}\right). \tag{28}$$

The obvious choice of fitting function, $J_1/J_0=(\beta-1)x^{-\beta}$ where β is an adjustable parameter, gives, unfortunately, poor results. Thus, we employed a power series function with 6 parameters as a fitting function:

$$\frac{J_1}{J_0} = \sum_{i=1}^{6} \frac{\gamma_i}{x^{2i}}. \tag{29}$$

The fitting parameters are presented in Table 2. All fitting functions give excellent agreement with the simulation data, as shown in Fig. 8.

Table 2. Fitting parameters of Eq. (29) at different values of N_G

N_G	γ_1	γ_2	γ_3	γ_4	γ_5	γ_6	Fitting range
1	−0.00603	0.38445	6.1641	−13.318	12.876	−4.6776	1<x<8.2
2	0.000731	−0.25649	8.343	−13.445	10.582	−3.4339	1<x<5.85
5	0.001384	−0.17534	0.52807	15.639	−21.504	8.0907	1<x<3.3
10	−0.1668	2.9108	19.345	54.562	−46.103	11.827	1<x<2.42
20	−1.2204	12.361	−42.711	48.262	12.909	−24.226	1<x<1.72
30	1.1751	−19.62	116.44	−315.85	387.22	−162.52	1<x<1.53
40	15.073	−157.17	642.43	−1277.7	1219.2	−433.67	1<x<1.47
50	60.963	−546.99	1936.3	−3364.2	2844.8	−921.43	1<x<1.50
100	1384.1	−9969.4	28442	−40114	27906	−7633.4	1<x<1.29

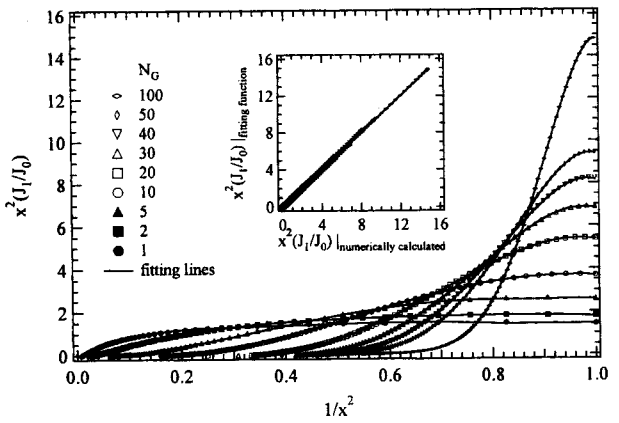

Fig. 8. Comparison of the fitting functions (29) with numerical results calculated at various values of N_G.

CONCLUSIONS

The convective-diffusion equation is useful for calculating the particle concentration profile and the rate of deposition over collector surfaces in a variety of deposition systems. While the convective-diffusion equation has been previously used to calculate the adsorption rate of particles on the bare surface [Elimelech, 1994a, 1994b], it has been extended here to the calculation of the particle flux distribution in the *presence of a preadsorbed particle.* First of all, convective-diffusion equations have been formulated in both 1+1 and 2+1 dimensional polar coordinate systems and solved for the 1+1 dimensional case by a collocation method. When the convection due to gravity dominates the diffusion due to molecular motion of particles, the concentration distribution of adsorbing particles shows a dramatic change from a slowly varying to a strongly biased distribution near the preadsorbed particle. From the concentration profiles particle flux distributions have been calculated at different N_G values and compared with the results of Brownian dynamics simulation. This comparison shows that the collocation method is accurate and more efficient than the Brownian dynamic simulation.

In this numerical study, we have also found that normalization based upon the concept of flux balance has allowed us to correct possible numerical errors due to the assumption of undisturbed boundary condition at an arbitrary position, $r=r_0$. Thus, when one numerically calculates particle flux distributions near a preadsorbed particle at high N_G values, one can overcome the difficulty of choosing appropriate system boundary because each numerical solution can be transformed to the correct distribution by normalization.

Finally, we have developed a truncated power series with 6 parameters as a fitting function which provides a good fit to the numerical solutions. This fitting function can be used to generate the structure of particle deposits on the line. As we did before elsewhere for $N_G=0$ [Thompson and Glandt, 1992], one can obtain the probability distribution of particles adsorbing between two preadsorbed particles by superimposing the flux due to two isolated preadsorbed particles.

ACKNOWLEDGEMENT

The research reported in this paper was supported by the Chungnam National University under 1996 University Research Grant.

Appendix. Application of the Collocation Method

To solve Eq. (2), we used a collocation method. For the sake of convenience, we transformed the convective-diffusion equation from (r, θ)-coordinates to normalized $(\tilde{r}, \tilde{\theta})$-coordinates in 1+1 and 2+1 D systems:

$$\tilde{\theta}=\frac{2}{\pi}\theta,\quad \tilde{r}=\frac{r-1}{r_0-1}. \tag{A.1}$$

Now, the convective-diffusion equation can be written as

$$\frac{\partial^2\Psi}{\partial\tilde{r}^2}+f(\tilde{r},\tilde{\theta})\frac{\partial\Psi}{\partial\tilde{r}}+g(\tilde{r})\frac{\partial^2\Psi}{\partial\tilde{\theta}^2}+h(\tilde{r},\tilde{\theta})\frac{\partial\Psi}{\partial\tilde{\theta}}=0, \tag{A.2}$$

and, in the 1+1 D system,

$$f(\tilde{r},\tilde{\theta})=\left[\frac{1}{k+\tilde{r}}+\frac{N_G}{k}\sin\left(\frac{\pi}{2}\tilde{\theta}\right)\right], \tag{A.3}$$

$$g(\tilde{r})=\frac{1}{(k+\tilde{r})^2}\left(\frac{2}{\pi}\right)^2 \tag{A.4}$$

$$h(\tilde{r},\tilde{\theta})=\frac{N_G}{k(k+\tilde{r})}\cos\left(\frac{\pi}{2}\tilde{\theta}\right)\left(\frac{2}{\pi}\right) \tag{A.5}$$

where

$$k=\frac{1}{r_0-1}, \tag{A.6}$$

and, in the 2+1 D system,

$$f(\tilde{r},\tilde{\theta})=\left[\frac{2}{k+\tilde{r}}+\frac{N_G}{k}\sin\left(\frac{\pi}{2}\tilde{\theta}\right)\right], \tag{A.7}$$

$$h(\tilde{r},\tilde{\theta})=-\left[\frac{\tan\left(\frac{\pi}{2}\tilde{\theta}\right)}{(k+\tilde{r})^2}-\frac{N_G}{k(k+\tilde{r})}\cos\left(\frac{\pi}{2}\tilde{\theta}\right)\right]\left(\frac{2}{\pi}\right), \quad (A.8)$$

respectively, with the boundary conditions (in both 1D and 2D)

$$\frac{\partial\Psi}{\partial\tilde{r}}=-\frac{N_G}{k}\sin\left(\frac{\pi}{2}\tilde{\theta}\right)\Psi \quad \text{at } \tilde{r}=0 \quad \text{and } 0\le\tilde{\theta}\le1$$

$$\Psi=1-\exp\left[-N_G r_0\sin\left(\frac{\pi}{2}\tilde{\theta}\right)\right] \quad \text{at } \tilde{r}=1 \quad \text{and } 0\le\tilde{\theta}\le1$$

$$\Psi=0 \quad \text{at } \tilde{\theta}=0 \quad \text{and } 0\le\tilde{r}\le1$$

$$\frac{\partial\Psi}{\partial\tilde{\theta}}=0 \quad \text{at } \tilde{\theta}=1 \quad \text{and } 0\le\tilde{r}\le1. \quad (A.9)$$

The approximate solution of the above diffusion equation can be written as a linear combination of Lagrangian Polynomials such as

$$\Psi(\tilde{r},\tilde{\theta})=\sum_{j=1}^{m+2}l_j(\tilde{\theta})\sum_{j=1}^{n+2}l_i(\tilde{r})\Psi_{ij} \quad (A.10)$$

where

$$l_i(\tilde{r})=\prod_{k=1,k\neq i}^{n}\frac{\tilde{r}-\tilde{r}_k}{\tilde{r}_i-\tilde{r}_k} \quad (A.11)$$

and

$$l_j(\tilde{\theta})=\prod_{k=1,k\neq j}^{m}\frac{\tilde{\theta}-\tilde{\theta}_k}{\tilde{\theta}_j-\tilde{\theta}_k} \quad (A.12)$$

where n and m are the number of collocation points in **r**-direction and θ-direction, respectively. Let us denote

$$l_j(\tilde{r}_i)=L_{ij}, \qquad l_j(\tilde{\theta}_i)=L'_{ij}$$

$$\frac{\partial l_j(\tilde{r}_i)}{\partial\tilde{r}_i}=A_{ij}, \qquad \frac{\partial l_j(\tilde{\theta}_i)}{\partial\tilde{\theta}_i}=A'_{ij}$$

$$\frac{\partial^2 l_j(\tilde{r}_i)}{\partial\tilde{r}_i^2}=B_{ij}, \qquad \frac{\partial^2 l_j(\tilde{\theta}_i)}{\partial\tilde{\theta}_i^2}=B'_{ij} \quad (A.13)$$

Since the Lagrangian polynomial has the following property:

$$L_{ij}=\begin{cases}0, & \text{if } i\neq j\\ 1, & \text{if } i=j\end{cases} \quad (A.14)$$

we can replace the partial derivatives of Eq. (A.2) with linear combinations of Lagrangian polynomials:

$$\Psi(\tilde{r}_k,\tilde{\theta}_l)=\sum_{j=1}^{m+2}\sum_{i=1}^{n+2}L'_{lj}L_{ki}\Psi_{ij}=\Psi_{kl} \quad (A.15)$$

$$\frac{\partial\Psi(\tilde{r}_k,\tilde{\theta}_l)}{\partial\tilde{r}}=\sum_{j=1}^{m+2}\sum_{i=1}^{n+2}L'_{lj}A_{ki}\Psi_{ij}=\sum_{i=1}^{n+2}A_{ki}\Psi_{il} \quad (A.16)$$

$$\frac{\partial^2\Psi(\tilde{r}_k,\tilde{\theta}_l)}{\partial\tilde{r}^2}=\sum_{i=1}^{n+2}B_{ki}\Psi_{il} \quad (A.17)$$

$$\frac{\partial\Psi(\tilde{r}_k,\tilde{\theta}_l)}{\partial\tilde{\theta}}=\sum_{j=1}^{m+2}A'_{lj}\Psi_{kj} \quad (A.18)$$

$$\frac{\partial^2\Psi(\tilde{r}_k,\tilde{\theta}_l)}{\partial\tilde{\theta}^2}=\sum_{j=1}^{m+2}B'_{lj}\Psi_{kj} \quad (A.19)$$

Substituting Eq. (A.15)-(A.19) into Eq. (A.2), we can construct the residual function $R(\tilde{r},\tilde{\theta})$:

$$R(\tilde{r}_k,\tilde{\theta}_l)=\sum_{i=1}^{n+2}[B_{ki}\Psi_{il}+f(\tilde{r}_k,\tilde{\theta}_l)A_{ki}\Psi_{il}]+\sum_{j=1}^{m+2}[g(\tilde{r}_k)B'_{lj}\Psi_{kj}+h(\tilde{r}_k,\tilde{\theta}_l)A'_{lj}\Psi_{kj}]. \quad (A.20)$$

And the boundary conditions can be written as follows:

$$\frac{\partial\Psi(\tilde{r}_1,\tilde{\theta}_l)}{\partial\tilde{r}}+\frac{N_G}{r}\sin\left(\frac{\pi}{2}\tilde{\theta}_l\right)\Psi=\sum_{i=1}^{n+2}A_{1i}\Psi_{il}+\frac{N_G}{k}\sin\left(\frac{\pi}{2}\tilde{\theta}_l\right)\Psi_{1l}=0$$

$$\Psi(\tilde{r}_{n+2},\tilde{\theta}_l)=1-\exp\left[-N_G r_0\sin\left(\frac{\pi}{2}\tilde{\theta}_l\right)\right]$$

$$\Psi(\tilde{r}_k,\tilde{\theta}_1)=0$$

$$\frac{\partial\Psi(\tilde{r}_k,\tilde{\theta}_{m+2})}{\partial\tilde{\theta}}=\sum_{j=1}^{m+2}A'_{n+2,j}\Psi_{kj}=0. \quad (A.21)$$

After inserting the boundary conditions Eq. (A.21) into Eq. (A. 20) and rearranging it, we finally obtain the following algebraic equation:

$$R(\tilde{r}_k,\tilde{\theta}_l)=\sum_{i=2}^{n+1}\left[B_{ki}-B_{k1}\frac{A_{1i}}{\alpha_{11}}+f(\tilde{r}_k,\tilde{\theta}_l)\left(A_{ki}-A_{k1}\frac{A_{1i}}{\alpha_{11}}\right)\right]\Psi_{il}+\sum_{j=2}^{m+2}\left[g(\tilde{r}_k)\left(B'_{lj}-B'_{l,m+2}\frac{A'_{m+2,j}}{A'_{m+2,m+2}}\right)+h(\tilde{r}_k,\tilde{\theta}_l)\left(A'_{lj}-A'_{l,m+2}\frac{A'_{m+2,j}}{A'_{m+2,m+2}}\right)\right]+D(\tilde{r},\tilde{\theta}) \quad (A.22)$$

where

$$D(\tilde{r},\tilde{\theta})=\left[\left(B_{k,n+2}-B_{k1}\frac{A_{1,n+2}}{\alpha_{11}}\right)+f(\tilde{r}_k,\tilde{\theta}_l)\left(A_{k,n+2}-A_{k1}\frac{A_{1,n+2}}{\alpha_{11}}\right)\right]\left[r_0\sin\left(\frac{\pi}{2}\tilde{\theta}_l\right)\right] \quad (A.23)$$

and

$$\alpha_{11}=A_{11}+\frac{N_G}{k}\sin\left(\frac{\pi}{2}\tilde{\theta}_l\right). \quad (A.24)$$

NOMENCLATURE

BD : ballistic deposition
c : particle concentration in the solution phase
c_o : particle concentration in the bulk phase

d : diameter of a particle
D : diffusion coefficient
DRSA : diffusion random sequential adsorption
F : force vector acting on a particle
I_a : area of integration under curves in Fig. 5
J(r) : flux at position r on the surface
J_1 : flux distribution due to the effect of a preadsorbed particle
J_0 : flux on an empty surface
k : Boltzmann constant
n_c : number of collocation point
N_G : dimensionless gravity number
N_{Pe} : Peclet number
N_S : sedimentation number
P : probability for jumping of a particle from its position to one of adjacent positions
r : position on the surface relative to the center of the preadsorbed particle
RSA : random sequential adsorption
T : temperature of system
x, y, z : Cartesian coordinate axes

Greek Letters

δ : jump distance
θ_∞ : saturation coverage of adsorbed particles
Ψ : normalized concentration distribution of particles in solution phase
Ψ_0 : steady state distribution of particles when the surface is empty
Ψ_1 : distribution due to the effect of a preadsorbed particle

REFERENCES

Andrade, J. D. and Hlady, V., "Protein Adsorption and Materials Biocompatibility", *Adv. Polymer Sci.*, **79**, 1 (1987).

Andrade, J. D., "Principles of Protein Adsorption", Surface and Interfacial Aspects of Biomolecular Polymers (Edited by Andrade, J.D.), Vol. 2, Protein Adsorption, Plenum Press, New York, 1985.

Andrade, J. D., "Thin Organic Films of Proteins", *Thin Solid Films*, **152**, 335 (1987).

Bafaluy, F. J., Choi, H. S., Senger, B. and Talbot, J., "Effect of Transport Mechanisms on the Irreversible Adsorption of Large Molecules", *Phys. Rev. E*, **51**, 5985 (1995).

Choi, H. S., Talbot, J., Tarjus, G. and Viot, P., "First-Layer Formation in Ballistic Deposition of Spherical Particles: Kinetics and Structure", *J. Chem. Phys.*, **99**, 9296 (1993).

Choi, H. S., "Irreversible Adsorption of Macromolecules at the Solid-Liquid Interface: Simulation and Theory", Ph.D. diss., Purdue University, West Lafayette, IN, USA (1995).

Elimelech, M., "Effect of Particle Size on the Kinetics of Particle Deposition under Attractive Double Layer Interactions", *J. Colloid Interface Sci.*, **164**, 190 (1994a).

Elimelech, M., "Particle Deposition on Ideal Collectors from Dilute Flowing Suspensions", *Sep. Technol.*, **4**, 186 (1994b).

Feder, J., "Random Sequential Adsorption", *J. Theor. Biol.*, **87**, 237 (1980).

Hinrichsen, E. L., Feder, J. and Jøssang, T., "Geometry of Random Sequential Adsorption", *J. Stat. Phys.*, **44**, 793 (1986).

Onoda, G. Y. and Liniger, B. G., "Experimental Determination of the Random Parking Limit in Two Dimensions", *Phys. Rev. Lett.*, **73**, 114 (1986).

Pagonabaraga, J. and Rubí, J. M., "Influence of Hydrodynamic Interactions on the Adsorption Process of Large Particles", *Phys. Rev. Lett.*, **73**, 114 (1994).

Schaaf, P. and Talbot, J., "Kinetics of Random Sequential Adsorption", *Phys. Rev. Lett.*, **62**, 175 (1989).

Senger, B., Bafaluy, F. J., Schaaf, P., Schmitt, A. and Voegel, J.-C., "Configurations of Adsorbed Hard Spheres after Diffusion in a Gravitational Field", *Proc. Nat. Acad. Sci.*, **89**, 9449 (1992).

Senger, B., Ezzeddin R., Bafaluy, F. J., Schaaf, P., Cuisinier, F. J. G. and Voegel, J.-C., "Influence of Diffusion and Gravity on the Adhesion of a Two-component Mixture of Hard Spheres on a Flat Surface", *J. Theor. Biol.*, **163**, 457 (1993).

Senger, B., Schaaf, P., Voegel, J.-C., Johner, A., Schmitt, A. and Talbot, J., "Influence of Bulk Diffusion on the Adsorption of Hard Spheres on a Flat Surface", *J. Chem. Phys.*, **97**, 3813 (1992).

Senger, B., Talbot, J., Schaaf, P., Schmitt, A. and Voegel, J.-C., "Effect of the Bulk Diffusion on the Jamming Limit Configurations for Irreversible Adsorption", *Europhys. Lett.*, **21**, 135 (1993).

Senger, B., Voegel, J.-C., Schaaf, P., Johner, A., Schmitt, A. and Talbot, J., "Properties of Jamming Configurations Built up by the Adsorption of Brownian Particles onto Solid Surfaces", *Phys. Rev. A*, **44**, 6926 (1991).

Slattery, J. C., "Momentum, Energy and Mass Transfer in Continua", McGraw-Hill, New York (1981).

Talbot, J. and Ricci, S., "Analytic Model for a Ballistic Deposition Process", *Phys. Rev. Lett.*, **68**, 958 (1992).

Thompson, A. P. and Glandt, E. D., "Low-coverage Kinetics of Correlated Sequential Adsorption", *Phys. Rev. A*, **46**, 4639 (1992).